

Supporting Information

***In-situ* assembled titanium carbide-based heterojunctions for synergistic enhancement of NIR-II photothermal/photodynamic therapy against breast cancer**

Hai Zhu, Xuequan Zhang, Qiusheng Wang, Jing Li, Jin Deng, Zhuangzhuang Zhang, Xiaoxian Zhang, Jun Cao*, Bin He*

*Corresponding authors:

Prof. Jun Cao, Bin He

National Engineering Research Center for Biomaterials, College of Biomedical Engineering, Sichuan University, Chengdu 610064, China

Tel: +86-28-85412848; E-mail: caojun@scu.edu.cn (J. C), bhe@scu.edu.cn (B.H)

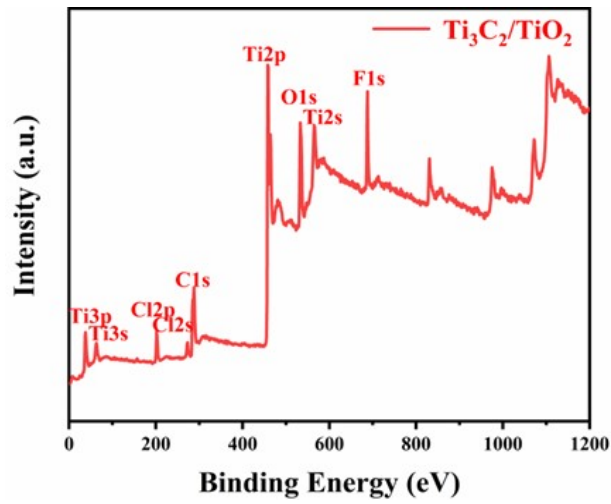


Fig. S1. XPS spectrum $\text{Ti}_3\text{C}_2/\text{TiO}_2$ in Ti 2p region.

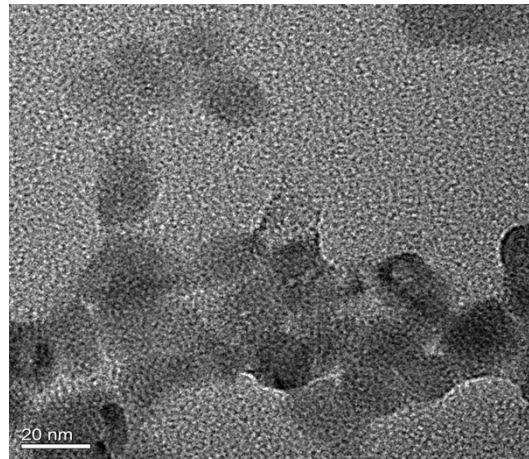


Fig. S2. The morphology of TiO_2 nanoparticles.

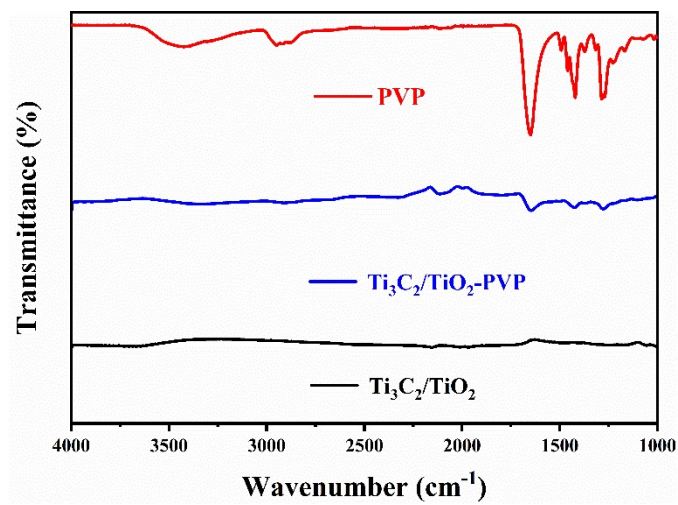


Fig. S3. FTIR spectra PVP, $\text{Ti}_3\text{C}_2/\text{TiO}_2$ and $\text{Ti}_3\text{C}_2/\text{TiO}_2$ -PVP HJs.

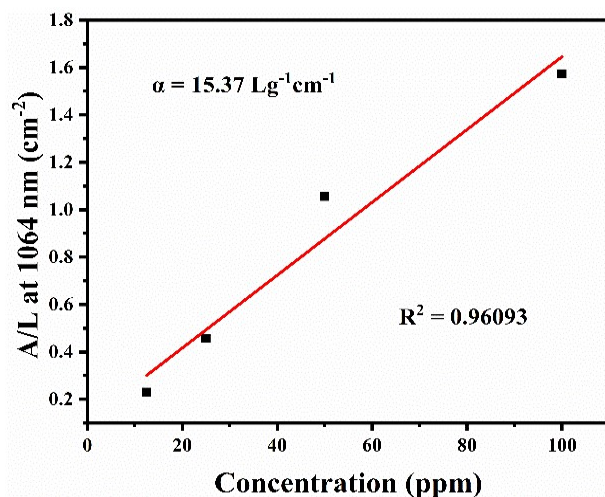


Fig. S4. Mass extinction coefficient of $\text{Ti}_3\text{C}_2/\text{TiO}_2$ -PVP HJs at 1064 nm.

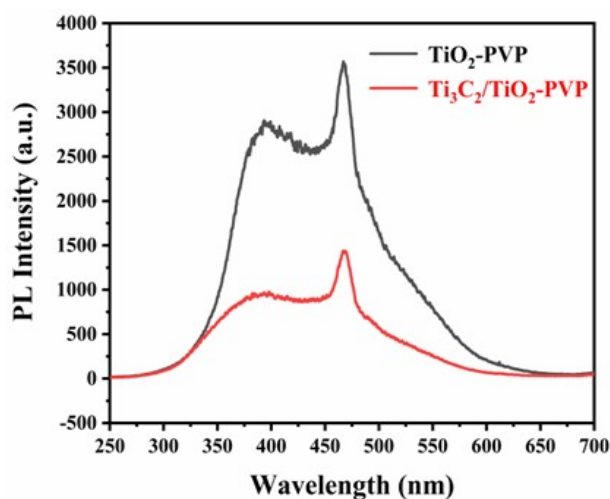


Fig. S5. Fluorescence spectra of TiO_2 -PVP and $\text{Ti}_3\text{C}_2/\text{TiO}_2$ -PVP HJs with the same titanium concentration.

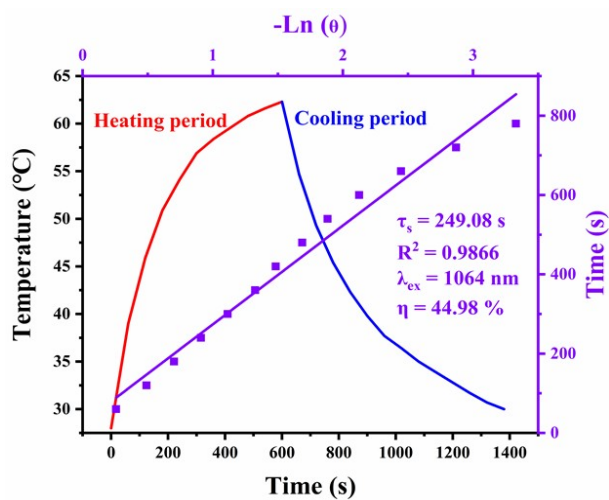


Fig. S6. Calculation of the photothermal-conversion efficiency at 1064 nm (NIR-II). Orange and blue line: photothermal effect of an aqueous dispersion of $\text{TiO}_2/\text{Ti}_3\text{C}_2$ -PVP

under the irradiation with NIR-II laser for certain periods, and then the laser was switched off. Purple line: time constant (τ_s) for the heat transfer from the system determined by applying the linear time data from the cooling period.

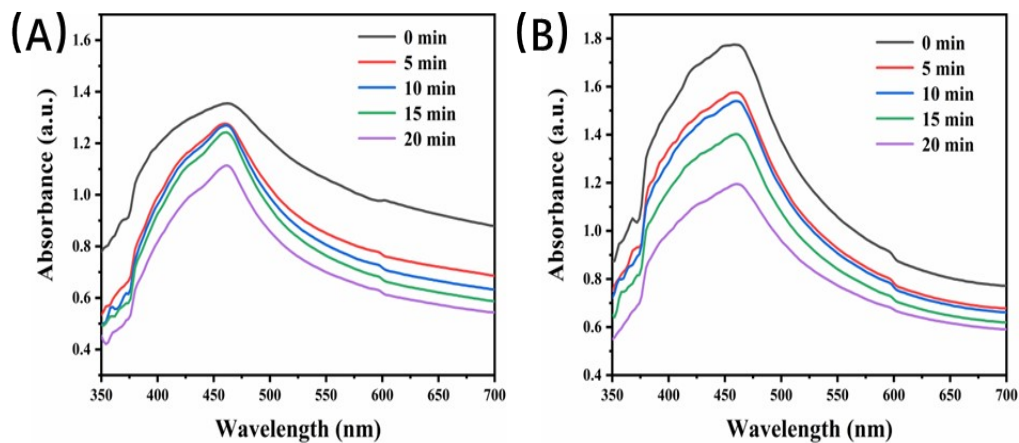


Fig. S7. Time-dependent degradation of DPBF caused by $^1\text{O}_2$ generated by TiO_2 -PVP (A) and Ti_3C_2 -PVP (B), respectively, under laser irradiation (660 nm, 1 W/cm², 10 min).

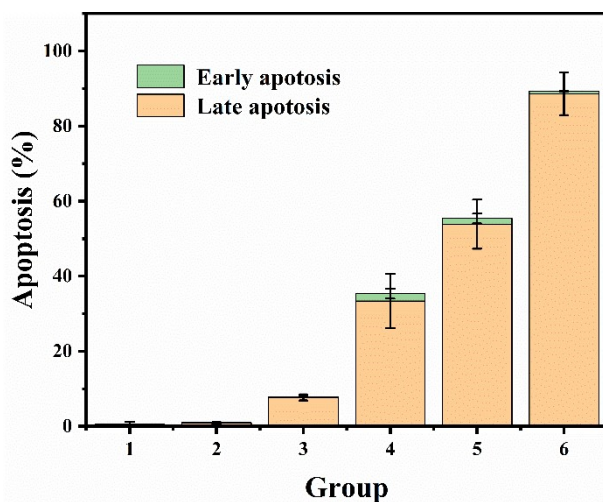


Fig. S8. Cell apoptosis of 4T1 cells after incubated with 0 and 200 ppm concentrations of $\text{Ti}_3\text{C}_2/\text{TiO}_2$ -PVP HJs with 1064 nm irradiation. Note: 1: Control; 2: Only 660 nm; 3: Only 1064 nm; 4: $\text{Ti}_3\text{C}_2/\text{TiO}_2$ -PVP+660 nm; 5: $\text{Ti}_3\text{C}_2/\text{TiO}_2$ -PVP+1064 nm; 6: $\text{Ti}_3\text{C}_2/\text{TiO}_2$ -PVP+660 nm+1064 nm.

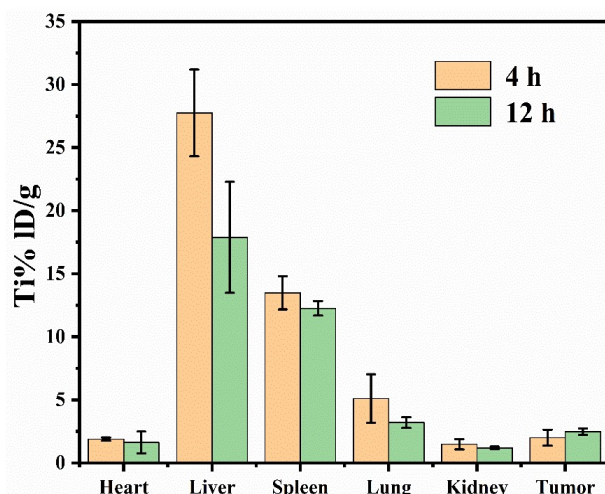


Fig. S9. In vivo Ti bio-distributions after injecting $\text{Ti}_3\text{C}_2/\text{TiO}_2$ -PVP into female tumor-bearing mice for 4 h, 12 h. Data are expressed mean \pm SD (n = 3).

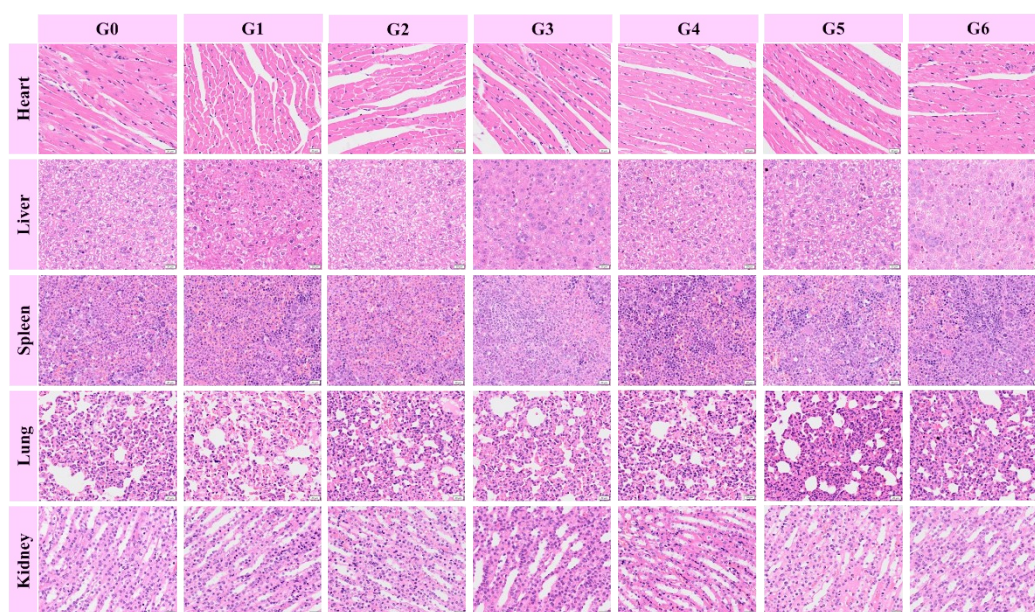


Fig. S10. H&E staining of heart, liver, spleen, lung and kidney from different groups (scale bar = 20 μm). Note: G0: control group (treated only with PBS), G1: 1064 nm laser group (only exposed to 1064 nm laser irradiation), G2: 660 nm laser group (only exposed to 660 nm laser irradiation), G3: $\text{Ti}_3\text{C}_2/\text{TiO}_2$ -PVP HJs group (only intravenously injected with $\text{Ti}_3\text{C}_2/\text{TiO}_2$ -PVP HJs), G4: $\text{Ti}_3\text{C}_2/\text{TiO}_2$ -PVP HJs + 660 nm laser group, G5: $\text{Ti}_3\text{C}_2/\text{TiO}_2$ -PVP HJs + 1064 nm laser group, and G6: $\text{Ti}_3\text{C}_2/\text{TiO}_2$ -PVP HJs + 660 and 1064 nm laser group.